Neuro Slicer: A Tool of Registering 2-D Slice Data to 3-D Surface Atlases

Bijan Timsari, Richard M. Leahy, Jean-Marie Bouteiller, and Michel Baudry
University of Southern California Brain Project, University of Southern California, Los Angeles, California

Abstract

In this article, we present a novel method for accurate registration of autoradiographs of rat brain to a standard atlas. This method minimizes the errors produced by nonlinear deformations of experimental samples and decreases the distortions caused by possible differences in the orientation and level of the sections between the experimental specimen and the reference brain. We have created a three-dimensional (3-D) surface atlas based on the two-dimensional (2-D) cryosection images used as reference maps of the rat brain. The surface can be resliced into new sections with a resolution high enough to cover a wide range of sectioning angles for experimental brains. Shape matching and transformation from sample data to the atlas is performed by using the Thin Plate spline model.

4.4.1 Introduction

Today, many clinical applications rely on medical imaging. Disease diagnosis, therapy planning, and surgical operations are often supported by several imaging modalities providing complementary information. There are many instances in which it would be desirable to integrate the information obtained from different studies on the same subject or similar studies on different subjects. Medical image matching is a difficult task, owing to the distinct physical realities represented by the imaging modalities, the differences in patient positioning, and the varying image acquisition parameters. Image registration is the fundamental task required for comparing two or more images acquired at different times, from different sensors, or from different subjects. What is usually referred to as *registration* is the process of spatially aligning two images by transforming the coordinates of each point in one image into the coordinates of the (physically) corresponding point in the other one. The determination of the optimal registration method depends on the types of variations between the images. In the literature, a broad range of methods for image registration has been proposed for various types of data and problems. This broad spectrum of methodologies makes it difficult to classify and compare techniques, as each technique is often designed for a specific application and not necessarily for specific types of problems or data. In recent years, a few surveys on registration methods in general image processing systems (Brown, 1992) and those with application in medical imaging (Maintz and Viergever, 1998; Maurer and Fitzpatrick, 1993; van den Elsen, 1994) have been published. More focused surveys with special attention to brain imaging have also been prepared (Thompson and Toga, 1999).

In general, the type of transformation used to register images is one of the best ways to categorize the methodology and select a technique for a particular application. In this context, a transformation is defined as a

mapping between two images both spatially and with respect to intensity, which may either act on the entire image as a whole (global mapping) or on the regions of the image based on their spatial locations (local mapping). The required characteristics of the transformation class used in the image registration paradigm are dictated by the specifics of the problem at hand. In situations where the relative size or shape of image components is to be retained, a rigid body transformation (a combination of rotation, translation, and scale change) is all that is required. Additionally, if shearing (a non-orthonormal rescaling operation) also needs to be accounted for, an affine transformation must be used. Affine transformations preserve parallelism between lines, but not necessarily their lengths. In more general cases, where the straightness of the lines is guaranteed to be preserved but parallelism between them is in general not preserved, a projective (or perspective) transformation must be used. Projective mappings account for distortions due to the projection of the objects at varying distances from the sensor onto the image plane. The most general class of transformations is elastic mappings. Elastic mappings are appropriate for problems that map straight lines into curves. Most elastic transformations try to conform to a set of physical constraints such as continuity, smoothness, and minimal energy state.

While the characteristics of the appropriate transformation class for a particular image registration problem are determined by the functional specifications of the mechanism responsible for image variations, the dimensionality of the transformation function is determined by the dimensions of the input and output image datasets. Image registration may be performed in any dimension, whether all dimensions are spatial or time is an added dimension. One-dimensional registration problems are exclusively used for performing temporal match on a time series of spatially consistent images. Two-dimensional methods may apply to intrinsically 2-D images, projection images, or separate slices from tomographic data. On the other hand, 3-D methods apply to tomographic images as a volumetric dataset not as a set of individual slices. In both case the matching procedure may include time as an extra dimension. Compared with 3-D to 3-D registration methods, 2-D to 2-D registration is far less complex, but it relies on an implicit assumption that the images to be matched are made exactly in the same plane with respect to a reference coordinate system. To meet this assumption, special provisions are required to ensure correct positioning of the object with respect to the imaging sensors. Even with the complicated imaging protocols these requirements demand, for some applications such as tomographic medical imaging the accuracy is rarely sufficient for 2-D to 2-D methods; therefore, most of the algorithms proposed for registration of tomographic datasets are 3-D to 3-D. In the literature, the class of 2-D to 3-D registration techniques is generally reserved for applications concerning direct alignment of spatial data to projective data (e.g., a pre-operative CT image to an intra-operative X-ray image) or the alignment of a single tomographic slice to spatial data (Maintz and Viergever, 1998).

In this article, we will study the problem of registering autoradiographic slice images of rat brain to a cryosection imaging based atlas. To solve this problem, we constructed a 3-D surface atlas from the available reference slice images and then resliced the reconstructed surface to generate new reference sections. Final registration is performed using a 2-D to 2-D technique; however, because the overall matching is between a 2-D image and a 3-D surface, this method can be categorized as a 2-D to 3-D method. Before we get into the detailed description of the USC Brain Project histological image registration tools we will quickly review different classes of image registration techniques that are currently used for medical images in general and brain images in particular to provide the reader with a general understanding of available methodologies along with their specific strong and weak points.

4.4.2 Classification Criteria

Registration methods are developed for a wide variety of applications and based on considerably different assumptions. Various discerning criteria have been proposed for classification of these methods (Maintz and Viergever, 1998). We have chosen a subject-based classification scheme to categorize registration methods into two classes: intrasubject and intersubject. The scope of our classification is restricted to methods that register brain images, and it covers all different brain imaging modalities. To keep our study brief, for each category we have selected for review only those methods that represent the dominant strategies in medical image registration (i.e., model-based approaches and intensity-based approaches).

As a common characteristic, all model-based algorithms are based on identifiable features of a geometric model of the brain. These explicitly defined features of the model correspond to anatomically significant elements of the brain, such as functionally important surfaces, curves, and point landmarks. Anatomical elements are matched with their counterparts, and their correspondences guides the transformation of one brain to another.

Intensity-based approaches use some statistical criteria to match the regional intensity patterns of the two images. Typically, the matching problem is cast as a problem in optimization theory for finding a transformation function that maximizes some mathematical measure of similarity between the deforming image and target. Measures of intensity similarity can include squared differences in pixel intensities, regional correlation, or mutual information.

4.4.3 Intrasubject Image Matching

When the goal of the registration task is to match the images acquired from a single subject at different times and under various conditions it is referred to as *intrasubject registration*. Such matches can occur within a given modality or between modalities. The most straightforward case is when the datasets are obtained using the same modality and the matching is accomplished by a linear transformation amounting to rotation and translation of the dataset. Another component may possibly be required for scaling to allow for the adjustment of size while maintaining shape as invariant. The result is a nine-parameter fit (rotation, translation, and scaling along each of the three spatial axes).

The problem of intrasubject, cross-modality registration is more difficult because of the modality-specific inconsistencies between images, such as incomplete coverage, intensity distortions, geometric distortions, and lack of contrast. One of the most common applications of intrasubject registration used in almost any type of diagnostic and interventional procedure is to match anatomical structures of the brain obtained from magnetic resonance imaging (MRI) with the physiological activities of each brain structure acquired from positron emission tomography (PET).

Model-Based Strategies

Point Pairs Matching

In the literature, a variety of techniques for mapping one brain to another using correspondences between homologous point landmarks have been described. The diversity of methods originates from the level of user interaction in identification of landmarks and the approach chosen for matching corresponding pairs of points. A well-known technique to solve 3-D rigid point to point match is using singular value decomposition (SVD) to find a transformation that minimizes the root mean square distance between homologous points in two datasets. Evans *et al.* (1991) apply this method to PET and MR brain images, while Hill *et al.* (1991) use it to register computerized tomography (CT) and MR skull base images. For the images that are misaligned by small rigid or affine transformations, cross-correlation can be used as a match metric to give a measure of the degree of similarity between two images. Maguire *et al.* (1986, 1991) used user-identified anatomical landmarks and external markers to find the affine transformation between tomographic brain images by optimizing the cross-correlation in areas around the landmarks.

Another frequently used approach is based on moment matching. From the moments of inertia, the principal axes of the object can be derived. Translation is found based on the position of the centroid of landmarks after equating the first-order moments. Rotation is calculated by aligning the landmark population's principal axes of inertia or equating the second-order moments. Calculating scaling factors is also possible from the relative magnitude of the principle axes (Alpert *et al.*, 1990; Bajcsy and Kovacic, 1989; Kovacic *et al.*, 1989).

Curve Matching

Curves, both in 2-D and 3-D, have been used as the basic feature for developing several image-matching algorithms. Matching curves without well-defined starting and ending points is the major bottleneck in most of these algorithms. Balter *et al.* (1992) first determine the overlap between corresponding curves by searching for the best fit of the local curvatures along the curves. From the overlapping segments, a number of point pairs are generated that are used in a direct point to point matching algorithm. Gueziec and Ayache (1992) make a table for all the curves in one image, with an index on their curvature and torsion parameters. Votes for particular transformations are generated by scanning the curvature and torsion parameters in the second image. From these votes a single rigid transformation is generated.

Surface Matching

A number of methods employ parametric correspondence between brain surface models extracted from tomographic images for matching them. The most popular method in this category is the "head-hat" surface matching technique (Pelizzari *et al.*, 1989) which tries to find a rigid (optionally affine) transformation that optimally fits a set of points (*hat*) extracted from the contours in one image to the surface model (*head*) extracted from another image. The *hat* fits the *head* when the mean squared distance between the *hat* points and the *head* surface is minimized.

Intensity-Based Strategies

Intensity-based approaches try to match the regional intensity patterns of the two images by comparing some statistical measure of similarity of the voxels. There are two distinct classes of approaches in this category. The first approach is to reduce image intensity content to a representative set of scalars and orientations from which the center of gravity and principal axes of the image will be calculated. Registration is then performed by aligning the center of gravity and the principal orientations (Alpert *et al.*, 1990; Banerjee and Toga, 1994). The second is to use the full image content throughout the registration process. Theoretically, these methods are more appealing because they use all of the available information for calculating the transformation function. The best example of this class of methods is registration based on minimization of variance of intensity ratios (Woods *et al.*, 1992, 1993). In this methodology, the rotation and translation parameters of the transformation function are adjusted iteratively by minimizing the

variance of the ratios between intensity values of all voxels in one image and a single voxel intensity value in the other.

4.4.4 Intersubject Image Matching

Intersubject registration is the task of matching two images belonging to different subjects. Despite the variations in size, orientation, topology, and geometric complexity of cortical and subcortical structures, the assumption underlying intersubject matching methods is that, at a certain level of representation, the topological structure of the brain is invariant among normal subjects (Rademacher *et al.*, 1993). The quantitative comparison of brain architecture across different subjects requires a structural framework in which individual brain maps can be integrated. "*Atlas*" is the general term used to refer to such a framework derived from either a single representative brain or an average anatomic template. The standardized 3-D coordinate system of the atlas (*stereotaxic* space) supplies a quantitative spatial reference system in which the variability of anatomical features from different individuals can be compared (Evans *et al.*, 1996) and multiple brain maps from different modalities can be correlated.

Brain Atlases

Classic atlases were developed based on a detailed representation of the individual anatomy of one brain (or a few brains) in a standardized 3-D coordinate system (Matsui and Hirano, 1978; Ono *et al.*, 1990; Paxinos and Watson, 1986; Schaltenbrand and Bailey, 1959; Schaltenbrand and Warren, 1977; Swanson, 1992; Talairach and Tournoux, 1988). Using these atlases generally involves employing simple proportional scaling systems to stretch or contract a given subject's brain to match the atlas. The classic 3-D neuroanatomic human atlases have proven to be useful for providing reference information required for stereotaxic surgical procedures (Kikinis *et al.*, 1996). However, as expected, such atlases are less accurate at brain sites with more intersubject variability and regions far from the landmarks of the reference system. To reflect the complex structural variability of individual brains the construction of brain atlases to represent large populations of subjects has become the focus of intensive research in recent years (Evans *et al.*, 1992; Friston *et al.*, 1995; Steinmetz *et al.*, 1989; van Buren and Maccubbin, 1962; Vries and McLinden, 1988).

Cryosection Imaging-Based Atlases

The purpose of cryosectioning is to collect high spatial imagery of the whole brain. Cryomacrotome sectioning of the frozen brain produces whole brain sections for staining and forms the basis of a reconstructed 3-D digital dataset. Frozen brains are usually sectioned in the coronal plane using a hardened steel knife, then the sections are photographed using digital imaging techniques. Several digital atlases have been developed using this method (Bohm *et al.*, 1983; Greitz *et al.*, 1991; Swanson 1992; Toga *et al.*, 1995).

Magnetic Resonance Imaging-Based Atlases

In recent years, development of a true 3-D atlas of the human brain has been made possible because of the growth in brain imaging technologies and the advances in development of 3-D segmentation methods. Consequently, for the first time in medical imaging history, anatomical details can be appreciated in 3-D instead of being restricted to 2-D images of 3-D structures. The major defect in MRI-based atlases is still the relatively low resolution and lack of anatomic contrast in important subregions. Where resolution is not a factor for development of an atlas, as in construction of population-based average atlases, MRI has proved to be very efficient (Andreasen *et al.*, 1994; Evans *et al.*, 1992). Average intensity atlases are useful for automated registration and mapping of MRI and fMRI datasets into stereotaxic space (Evans *et al.*, 1994).

Multi-Modality Atlases

In 1993, the U.S. National Library of Medicine funded a team of researchers under the Visible Human Project to produce thousands of razor-thin slices of two cadavers (male and female) which were photographed to capture detailed images of the structures in the body. The outcome was over 15 gigabytes of image data, including CAT scans, MRI, and cryosection images. Combining the strengths of each imaging modality, the Visible Human dataset, although not a brain atlas, has the quality and accessibility to be used as a test platform for developing methods and standards (Spritzer *et al.*, 1996).

Probabilistic Atlases

Due to the large variation in the anatomy of brain in different individuals, an atlas based on a single subject's anatomy cannot be a true representative of the whole population. To generate anatomical templates whose data can be extendable to a population, probabilistic atlases were introduced. These atlases contain precise statistical information on positional variability of important functional and structural organizations of the brain (Matsui and Hirano, 1978).

Model-Based Strategies

The first stage of any intersubject registration method is the transformation of individual data to the space occupied by the atlas. A stereotaxic coordinate system has been used conventionally as a framework for representing quantitative information about 3-D spatial relationships in the brain. The most widely used stereotaxic system introduced by Talairach (Talairach and Szikla,

1967; Talairach and Tournoux, 1988) is defined by a set of piece-wise affine transformations applied to 12 rectangular regions of brain, specified by drawing lines from the anterior and posterior commissures to the extrema of the cortex. Despite the widespread usage of Talairach stereotaxic system as a standard coordinate system for researchers to compare and contrast their results (Fox *et al.*, 1985; Friston *et al.*, 1991), the fact remains that linear transformations (rotation, scaling, translation) by themselves are not sufficient to remove the large intersubject structural variation in the anatomy of brain. Elastic transformations are required to adapt the shape of an atlas to reflect the anatomy of an individual subject.

Among model-based techniques, deformable models offer the unique characteristic of accommodating the significant variability of biological structures over time and across different individuals by combining geometry, physics, and approximation theory. Geometry serves to represent object shape, physics imposes constraints on how the shape may vary over space and time, and approximation theory provides the formal mechanism for finding an optimal model fitting the measured data. For broader shape coverage, deformable models usually employ geometric representations that involve many degrees of freedom, such as splines. The freedom of model is limited by physical principles that impose intuitively meaningful behavior on the geometric substrate. Physically, a deformable model can be viewed as an elastic body subject to a set of constraints which is responding naturally to a system of applied forces. An energy function defined in terms of the model's geometric degrees of freedom quantifies the deformation.

Point Pairs Matching

A global transformation derived from matching pairs of corresponding points on two images cannot account for local geometric deformations. In case of an approximating transformation, the local distortions are spread throughout the image, while for interpolating transformations high-order polynomials will usually be required, and these behave erratically. Piece-wise interpolation techniques based on point matching can account for deformations which vary across different regions of the image. In this methodology, a spatial mapping transformation is specified for each coordinate which interpolates between the matched coordinate values. Various choices of interpolating functions have been used for medical image matching, including thin-plate spline (Bookstein, 1989), 3-D volume spline (Davis *et al.*, 1997), elastic body spline (Davis *et al.*, 1997), and multiquadric and shifted log interpolants (Frank, 1979; Hardy, 1990; Ruprecht and Muller, 1995).

Curve Matching

Choosing the best feature space to use for matching will significantly improve the registration result. Structural similarity and as a result anatomical accuracy can be increased if matching is based on features extracted from intrinsic structures of the images. Edges, contours, and boundaries are frequently used as a feature space because they represent the intrinsic structure of an image. In recent years, several warping transformations based on lines and curves with salient features have been introduced (Declerck *et al.*, 1995; Joshi *et al.*,1995). Curve-matching algorithms try to match curves with their counterparts in the target image using geometric features such as torsion, curvature, and local Frenet frames as guiding parameters (Gourdon and Ayache, 1993; Kishon *et al.*, 1991; Vaillant and Davatzikos, 1997).

Surface Matching

A natural extension of matching techniques based on curve and line feature spaces is surface-based warping algorithms. Such algorithms warp one image to another by elastically deforming a surface extracted from the source dataset to its homologous surface in the target domain. The success of these methods depends on the accuracy of the surfaces they match. Several algorithms have been proposed for extracting brain surfaces from 3-D image volumes. The analytical form of the surface is calculated either directly by the extraction algorithm or in a later processing through a flattening procedure. Extraction algorithms that start with a parametric model for the surface and try to deform it to match a target boundary end up with an analytic form (MacDonald *et al.*, 1993; Vaillant and Davatzikos, 1997; Xu and Prince, 1997), while others create a segmented volume whose boundary defines the surface (Sandor and Leahy, 1995). The latter approach generally produces a more detailed and accurate description for the surface which may justify the cost of the additional flattening step required for obtaining its analytic description (Drury *et al.*, 1996). From the extracted surfaces represented in analytical form, warping functions can be computed to map surfaces from the atlas to the target image. To guide the mapping from atlas to target anatomically significant features of both objects are detected and forced to match (Collins *et al.*, 1996; Thompson and Toga, 1996). Deformable models that can accurately locate image features such as snakes and their extension have been successfully used for this purpose (Sandor and Leahy, 1995).

Intensity-Based Strategies

In many applications, it is desired to map data from a variety of modalities into an atlas coordinate space without requiring structural correspondence at a local level. With the development of average-intensity MRI atlases in the Talairach coordinate system, automated image registration algorithms have emerged for this purpose. These algorithms try to align new datasets with the atlas by maximizing a measure of intensity similarity, such as

3-D cross-correlation (Collins *et al.*, 1994, 1995) or ratio image uniformity (Woods *et al.*, 1992).

On the other hand, when the goal is perfect intersubject registration of brain data, the atlas must be deformed in an extremely local level to fit the shape of the target anatomy. This requires the warping transformation to be of high spatial dimension. Local deformations do not necessarily preserve the connectivity and topology of transformed objects. To ensure that the atlas will not break into parts under such complex transformations it is typically considered to be embedded in a 3-D deformable medium which can be either an elastic material (Bajcsy and Kovacic, 1989; Broit, 1981; Miller *et al.*, 1993) or a viscous fluid (Christensen *et al.*, 1994). All intensity-based approaches basically try to redistribute the image intensity in the atlas to make it more similar to the target. Different algorithms vary depending on how the similarity function is defined and maximized.

Elastic Medium Approaches

In this approach, a brain atlas modeled as an elastic medium is subject to two systems of opposing forces, external forces trying to deform the atlas and internal restoring forces generated by the elasticity of the mater ial. The displacement field at equilibrium state is described by the Navier-Stokes equation:

$$\mu\nabla^2 U(x) + (\lambda + \mu)\nabla(\nabla \cdot U(x)) + F(x) = 0 \quad \forall x \in R \tag{1}$$

where R is discrete lattice representation of the atlas,

$$\nabla \cdot U(x) = \sum_i \partial u_i / \partial x_i \tag{2}$$

shows the cubical dilation of the medium; ∇^2 is the Laplacian operator; λ and μ define the elastic properties of the body; $U = U(x_1, x_2, x_3)$ is the displacement field; and $F(x)$ is the external force. This system of partial differential equations can be solved iteratively on the defined lattice and interpolated trilinearly to obtain a continuous displacement field.

Viscous Fluid Approaches

Linear elastic models are valid only for small deformations. Restoring forces are proportional to the deformed distance and as a result the displacement field resulting from these forces is limited to be low in magnitude, leaving the atlas incompletely warped onto the target.Viscous fluid based models were developed to overcome this limitation of elastic models. The displacement field obtained from the solution to the elastic equilibrium equation is used as an initial value for the viscous fluid differential equation:

$$\alpha\nabla^2 V(x,t) + \beta\nabla(\nabla^t V(x,t)) = F(x) \tag{3}$$

where α and β are viscosity constants; $F(x)$ is the external deforming force (per unit volume); and $V(x,t)$ is the instantaneous velocity of the deforming atlas at location x at time t. The velocity, $V(x,t)$, is related to the displacement field, $U(x,t)$, by the equation:

$$V(x,t) = \frac{\partial U(x,t)}{\partial t} + V(x,t)\nabla \cdot U(x,t) \tag{4}$$

As the atlas deforms to match the target over time, the external force goes to zero, which causes the velocity to go to zero, and final match is obtained.

4.4.5 Neuro Slicer: USCBP Histological Registration Tool

Many biological measurements of the brain depend upon the qualitative evaluation of radiolabelled samples to provide information about protein metabolism, gene expression, and nucleic acid sequences. Quantitative analysis of autoradiographic data helps neuroscientists to determine the functional properties of a particular region in response to a given treatment or to obtain some knowledge about the mechanisms for expressing certain responses. Furthermore, integrating and comparing data from multiple subjects provides the researchers an understanding of the functional behavior and structural organization of the brain.

Most autoradiographic image data used in histological studies, though information rich and high resolution, present non-linear deformations due to specimen sectioning. These deformations together with natural morphological differences between individual brains make the task of comparing results from different studies more challenging. For a meaningful interpretation, when analyzing autoradiographic images, the data collected from multiple subjects should be compared with respect to some standardized base of reference. This requires an atlas of brain anatomy with the resolution of an autoradiogram, which considering the current state of imaging technology is limited to cryosection-imaging based atlases.

Ideally, the data in each experimental brain section must be mapped to the corresponding homologous section in the atlas, and all the quantitative measurements have to be made with respect to the atlas. Selection of homologous sections is traditionally done by an expert based on visual judgement. However, in the very likely situation when the orientation or position of the plane of sectioning of the experimental brain does not match that of the reference brain, this method is potentially error prone.

As an alternative, if instead of a series of 2-D cryosection images of brain, a 3-D atlas is used, then theoretically it would be possible to find homologous atlas sections for any given experimental brain section without any error. Based on this, we have developed a method for non-rigid registration of autoradiographic images of rat

brain using a 3-D surface atlas. Our approach is categorized in the class of model-driven, feature-point-based, 2-D to 3-D registration methods and comprises the following steps.

Reconstruction of Surface Atlas

Compared to 2-D atlases, a full 3-D atlas contains a spatially continuous description of the physical entity it is representing. Due to the limited resolution of current non-invasive 3-D medical imaging modalities which is far less than the resolution required for histological studies, 2-D cryosection imaging-based atlases are commonly used for such studies. Swanson's rat brain atlas (Swanson, 1992), one of the most comprehensive atlases of this type for rat brain, consists of 73 coronal (frontal or transverse) sections in which major cell groups and fiber tracts along with their subdivisions are labeled. In the structural hierarchy of this atlas gross segments, regions, cell groups, and fiber tracts are identified by their boundaries. Tissue labeling and region identification were both performed manually section by section. This has naturally caused loss of data continuity along the dorso-ventral axis. A sample section is displayed in Fig. 1. To restore the lost continuity, one can interpolate between the data in available sections. Depending on the desired accuracy, different interpolating functions can be used for this purpose.

In the digital version of Swanson's atlas, image data are conveniently stored in two formats: raster and vector. The raster file format is best for representing image intensity value at each voxel and is used when interpolating the cross-sectional density maps to create 3-D volume data. Vector format, on the other hand, is for representing curves and contours. All the information required to reconstruct surfaces by interpolating between curves is abstracted in this format. Although, for a quantitative study, the full 3-D form of both the volume and the surface are required, for the purpose of visualization one may choose only the surface atlas to take advantage of the speed and capabilities of the available surface rendering tools.

Reconstructing the surface of an object from a series of planar contours corresponding to the intersection of its boundary with a set of parallel planes is of major interest in computer-aided design of mechanical and architectural structures. Several general purpose and many custom-made programs have been developed for this purpose. We have used Microstation, one of the available commercial packages for solid modeling, drafting, and visualization of CAD products, for creating the 3-D surface of the labeled structures in Swanson's rat brain atlas.

The line drawings, marking the boundary contours of different structures in each one of the 73 sections of the atlas, were imported into this program in vector format. A bicubic B-spline model was then used to fit a parametric surface to a selected subset of these line drawings. The parametric model of the reconstructed surfaces can be easily used for calculating the cross-sectional profile of the surface within any arbitrary plane. Fig. 2 shows a sample surface reconstructed by this method. This surface represents the left half of rat brain cortex cut at the top to display the internal structures of the brain.

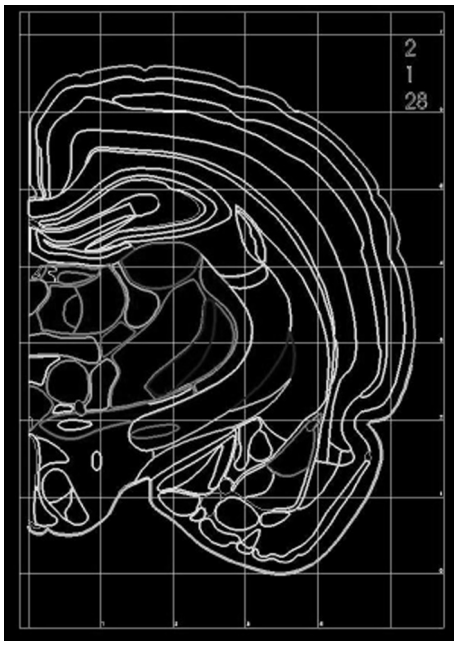

Figure 1 A sample section from Swanson's rat brain atlas. The contours represent the boundaries of the structures in the left hemisphere of rat brain.

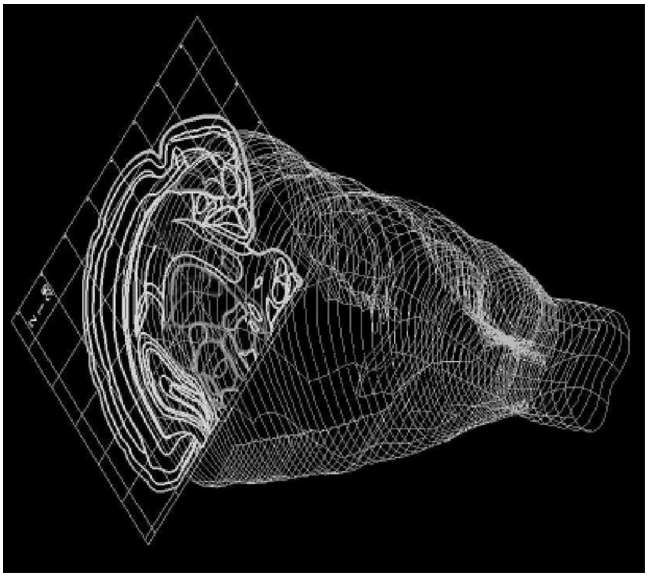

Figure 2 A wire-frame representation of the left half of the reconstructed rat brain cortex. The top part of the brain is removed to display internal structures.

Matching Experimental Data to Atlas

In histological studies, when the autoradiogram of an experimental specimen is to be compared with a standard atlas, classically, an expert selects a particular level of the atlas as the closest match for the experimental image. In this selection he uses his knowledge and experience to look for similar shape patterns between two images. The shape of an object is described by words or quantities that do not change when the object is moved, rotated, enlarged, or reduced. Mathematically, shape is defined as the geometric properties of a configuration of points that are invariant to changes in translation, rotation, and scale (Kendall, 1984). By quantifying shapes and defining a measure for shape distance one can automate the process of atlas matching.

Mathematically, shapes are defined as equivalence classes of discrete point sets, called *landmarks*, under the operation of Euclidean similarity transforms (Bookstein, 1991). Landmarks are labeled points on a biological image located according to some rule. Generally, on a biological image, landmarks are selected as a set of anatomically significant points that are easily identified across all images. The similarity between two landmark shapes is measured in terms of their Procrustes distance. Informally, the squared procrustes distance between two sets, A and B, of landmark points is the minimum sum of squared Euclidean distances between the landmarks of A and the corresponding landmarks in point sets C as C ranges over the whole set of shapes equivalent to B (Bookstein, 1991). To measure the shape distance between two point sets, first their centroids have to be translated to the origin of their common coordinate system. Then their centroid size, the square root of the summed squared distances between landmarks and their centroid, is scaled to unity. Finally, these scaled and translated images are superimposed at their centroid and one of them is rotated with respect to the other to minimize the sum of squares of the residual distances between matched landmarks. The squared Procrustes distance between the shapes is the sum of squares of those residuals at the minimum state (Bookstein, 1991).

The only nontrivial part of this algorithm is calculating the rotation required to superimpose the two images. Let X_1 and X_2 be $k \times 3$ matrices for the coordinates of k landmarks after the centering and re-scaling has been done. It can be shown (Rohlf, 1990) that if the singular-value decomposition of $X_1^t X_2$ is UDV^t with all elements of D positive, then the rotation required to superimpose X_2 upon X_1 is the matrix VU^t.

To avoid the computational cost of singular-value decomposition, one can use other methods to approximate Procrustes distances. We can use the notation of complex algebra to represent the two sets of landmark points by two complex vectors $Z_j = (Z_{1j}, Z_{2j}, \ldots, Z_{kj})^t$, $j = 1, 2$. After the centering and re-scaling steps, we have:

$$\sum_i Z_{ij} = 0 \quad (j = 1, 2) \tag{5}$$

$$\sum_i Z_{ij} Z_{ij}^* = 1 \quad (j = 1, 2) \tag{6}$$

where * denotes complex conjugate. The superposition of the second image on the first is given approximately by:

$$Z_2 \rightarrow (\sum_i Z_{i1} Z_{i2}^*) Z_2 \tag{7}$$

and the squared Procrustes distance between the two shapes is approximately (Bookstein, 1997):

$$D_p^2(Z_1, Z_2) = 1 - \left| \sum_i Z_{i1} Z_{i2}^* \right|^2 \tag{8}$$

Within this framework, matching an experimental image to the atlas is equivalent to finding a profile from the atlas with a configuration of landmarks similar to the experimental image. This is essentially a search for a particular pattern of 2-D feature points in a 3-D feature spaces. There is an inherent ambiguity involved in this process because the mapping between 3-D vectors and their projections in 2-D space is many to one. To remove this ambiguity one has to limit the search only to 2-D projection spaces. We have accomplished this with the following method.

A certain number of anatomically significant landmark points are selected and their locations are marked with small circles on the brain sections where they appear. These circles will form continuous cylindrical tubes after 2-D to 3-D interpolation is applied to consecutive sections of the brain. Fig. 3 shows the reconstructed landmark tubes in the portion of the brain that contains the hypocampus.

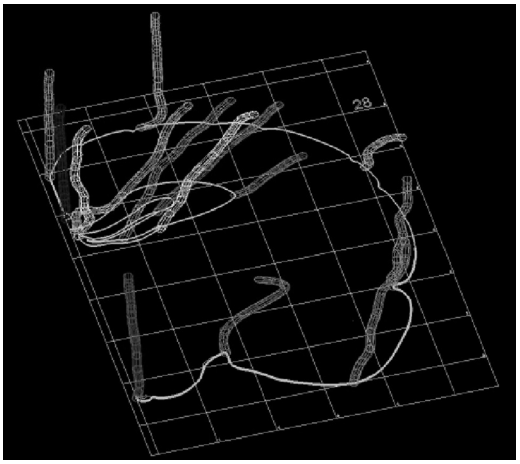

Figure 3 Landmarks marked with small circles on different sections of the brain form cylindrical tubes when reconstructed using a 2-D to 3-D interpolation technique.

Having a 3-D atlas with embeded labeled landmarks provides us the possibility of generating arbitrarily oriented reference sections with pre-labeled landmark points on them. By re-sectioning the 3-D atlas with a cutting plane with adjustable position and varying orientation, a set of 2-D profiles is formed. The collection of all profiles forms the search space for the matching algorithm. In order to get the desired spatial resolution and to cover the possible range of variation in the cutting angle of the experimental brain, re-sectioning is performed by making cuts in the coronal plane as well as planes rotating within the range of -10° to $+10^\circ$ (with increments of 0.5°) around medio-lateral and dorso-ventral axes. A 5–micron distance between two consecutive coronal planes appears to give sufficient spatial resolution for our purpose.

The same set of landmark points is correspondingly marked on experimental images. To match an experimental image to the atlas, the Procrustes distance between its landmark points and the profiles in the pool of atlas sections is calculated. The minimum distance determines the profile of the standard brain that is most similar to the experimental image. To speed up the search for the closest atlas profile, matching is broken down into several stages. The vicinity of the experimental section in the brain is determined using a search over the entire brain with relatively widely spaced profiles with large angular differences. Then, using higher resolution profiles, the margins are narrowed repeatedly until the best match is found.

Warping Experimental Image

In general, when the mapping between two images is guided by the specification of the correspondence between landmark points various deformation functions can be found that are consistent with the displacements assigned at landmark points. The ambiguity lies in the construction of the non-rigid part of the transformation after the correspondences between the first three pairs of landmarks are used for calculation of the rigid portion of the mapping. One way to resolve this ambiguity is to require the deformation field to have minimum irregularity or roughness by adding a regularizing functional to the mapping (Tikhonov and Arsenin, 1977). A regularizer function penalizes large values of derivatives and thus smooths the deformation field, but at the same time it should create warping transformations that satisfy displacement values at landmark points and do not vary erratically elsewhere.

Thin-plate splines are functions which minimize the penalty:

$$\left(\frac{\partial^2 Z}{\partial x^2}\right)^2 + 2\left(\frac{\partial^2 Z}{\partial xy}\right)^2 + \left(\frac{\partial^2 Z}{\partial y^2}\right)^2 \tag{9}$$

known as the bending energy of function,

$$Z(x,y) = -U(r) = -r^2 \log r^2 \tag{10}$$

over the class of all functions Z taking the specified displacement values at landmark points. A thin-plate spline function has a quadratic form in r, the distance $(x^2+y^2)^{1/2}$ from the origin of the Cartesian coordinate system, and is the fundamental solution of the biharmonic equation:

$$\Delta^2 U = \left(\frac{\partial^2}{\partial x^2} + \frac{\partial^2}{\partial y^2}\right)^2 U = 0 \tag{11}$$

the equation for the shape of a thin steel plate lofted as a function $Z(x,y)$ above the plane (x,y) (Bookstein, 1997). The mapping that extends the displacement field from a set of pairs of landmark points to the entire 2-D space is given by:

$$\begin{pmatrix} x' \\ y' \end{pmatrix} = A\begin{pmatrix} x \\ y \end{pmatrix} + T\begin{pmatrix} Z_x(x,y) \\ Z_y(x,y) \end{pmatrix} \tag{12}$$

where A represents a 2×2 linear transformation matrix, and T is the translation vector. The vector $Z = (Z_x, Z_y)$ represents the nonlinear part of the warping transformation defined by:

$$Z_\eta(x,y) = \sum_{i=1}^{N} \omega_{\eta i} U(\left|(x,y)^t - (x_i,y_i)^t\right|) \qquad \eta \in \{1,2\} \tag{13}$$

in which U is the thin-plate spline function. The unknown coefficients $\omega_{\eta i}$ along with the elements of matrix A and translation vector T are determined by evaluating the equation at the given landmark points $(x_i,y_i)^t$ and solving the resulting linear system of equations.

Results

We have created a 3-D atlas for the rat brain based on a series of maps originally generated by Swanson. We used vector representation of a subset of line drawings in the atlas, corresponding to the boundaries of different structures in the brain, to extract the location of their control points. These data were then used to describe the outer boundaries of the structures with a bicubic B-spline parametric surface model. Using the parametric model for the surface, we can easily calculate the cross-sectional profile of the surface within any arbitrary plane.

To describe the rat brain-shape information in terms of the configuration of a finite number of discrete points, we have identified a set of anatomically significant landmark points and manually marked them on each section of the atlas. When reconstructed, these landmarks form continuous tubes. The assembly of tubes constitutes a 3-D object with a shape equivalent to the atlas. A pool of profiles for the standard rat brain is generated by reslicing the 3-D atlas shape-equivalent object. To cover

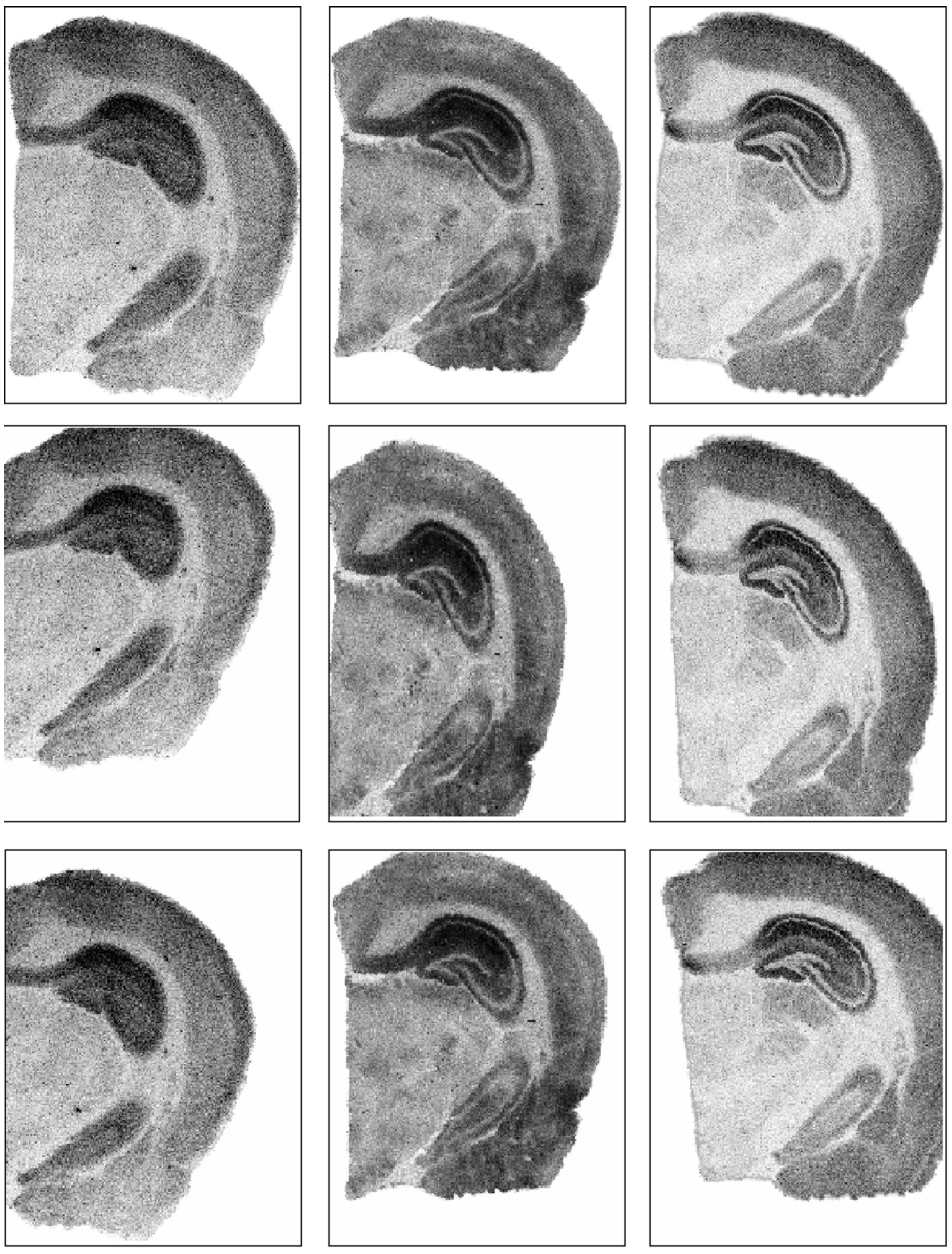

Figure 4 Performance of the proposed algorithm. (First row) Original experimental section. (Second row) Experimental section mapped to the best matching atlas section selected by an expert. (Third row) Experimental section mapped to the best matching atlas section found based on the proposed algorithm.

possible deviations in the cutting angle of experimental brain from that of standard brain, re-slicing is performed in steps of 5 microns and each step generates sections in the coronal plane as well as planes rotating within the range of -10 to $+10^{\circ}$ (with increments of 1°) around medio-lateral and dorso-ventral axes. The same set of landmark points is correspondingly marked and labeled on experimental images. To match an experimental image to the atlas, the Procrustes distance between its landmark points and the profiles in the pool of atlas sections is calculated. The minimum distance determines the profile of the standard brain that is most similar to experimental image.

A series of experiments was carried out to evaluate the performance of the algorithm. In each experiment, a sample section of a rat brain was mapped to the atlas using two different methods:

1. By following the classic method and using the original 2-D atlas, an expert was asked to select a section from the atlas which he found most similar to the experimental section.
2. By following the described algorithm, predefined landmark points were labeled on the experimental section and then the procrustes distance from the sections in the searching pool was calculated. The

best match in this case was the one having the shortest distance.

3. In both cases, the experimental section was mapped to its best match using thin-plate spline transformation.

All experiments showed that by using the second method we can gain significant improvements in the matching results. Fig. 4 show three sample results of these experiments. The first row shows the original image of experimental brain sections, the middle row is the result of warping the experimental images to atlas sections selected by an expert using thin-plate spline, and the last row shows the result of our registration/warping tool.

References

Alpert, N. M., Bradshaw, J. F., Kennedy, D., and Correia, J. A. (1990). The principal axis transformation a method for image registration. *J. Nucl. Med.* **31**, 1717–1722.

Amit, Y. (1997). Graphical shape templates for automatic anatomy detection with applications to MRI brain scans. *IEEE Trans. Med. Imag*. **16(1)**, 28–40

Andreasen, N. C., Arndt, S., Swayze, V., Cizadlo, T., Flaum, M., O'Leary, D., Ehrhardt, J. C., and Yuh, W. T. C. (1994). Thalamic abnormalities in schizophrenia visualized through magnetic resonance image averaging. *Science* **266**, 294–298.

Bajcsy, R., and Kovacic, S. (1989). Multiresolution elastic matching. *Computer Vision, Graphics, Image Processing* **1(46)**, 1–21.

Balter, J. M., Pelizzari, C. A., and Chen, G. T. Y. (1992). Correlation of projection radiographs in radiation therapy using open curve segments and points. *Med. Phys*. **19(2)**, 329–334.

Banerjee, P. K., and Toga, A. W. (1994). Image alignment by integrated rotational and translational transformation matrix. *Phys. Med. Biol*. **39**, 1969–1988.

Bohm, C., Greitz, T., Kingsley, D., Berggren, B. M., and Olsson, L. (1983). Adjustable computerized brain atlas for transmission and emission. *Tomography, Am. J. Neuroradiol*. **4**, 731–733.

Bookstein, F. L. (1997). Landmark methods for forms without landmarks, morphometrics of group differences in outline shape. *Med. Image Anal*. **1**, 225–243.

Bookstein, F. L. (1991). *Morphometric Tools for Landmark Data, Geometry, and Biology*. Cambridge University Press, New York.

Bookstein, F. L. (1989). Principal warps, thin-plate splines and the decomposition of deformations. *IEEE Trans. Pattern Analysis Machine Intelligence* **11(6)**, 567–585.

Broit, C. (1981). Optimal Registration of Deformed Images, Ph.D. thesis. University of Pennsylvania, Philadelphia.

Brown, L. G. (1992). A survey of image registration techniques. *ACM Computing Surveys*. **24(4)**, 325–376.

Christensen, G. E., Rabbitt, R. D., and Miller, M. I. (1994). 3-D brain mapping using a deformable neuroanatomy. *Phys. Med. Biol*. **39**, 609–618.

Collins, D. L., Neelin, P., Peters, T. M., and Evans, A. C. (1994). Automatic 3D intersubject registration of MR volumetric data into standardized Talairach space. *J. Comp. Assisted Tomography*. **18(2)**, 192–205.

Collins, D. L. Holmes, C. J., Peters, T. M., and Evans, A. C. (1995). Automatic 3D model based neuroanatomical segmentation. *Human Brain Mapping* **3**, 190–208.

Collins, D. L., Le Goualher, G., Venugopal, R., Caramanos, A., Evans, A. C., and Barillot, C. (1996). Cortical constraints for non-linear cortical registration. In *Visualization in Biomedical Computing* (Hohne, K. H. and Kikinis, R., Eds.). Lecture Notes in Computer Science. Vol. 1131. Springer-Verlag, Berlin, pp. 307–316.

Davatzikos, C., and Prince, J. L. (1996). Convexity analysis of active contour problems. In, *Proceedings of CVPR*. June 17–20, San Francisco, CA.

Davis, M. H., Khotanzad, A., Flaming, D. P., and Harms, S. E. (1997). A physics-based coordinate transformation for 3D image matching. *IEEE Trans. Med. Imaging* **16(3)**, 317–328.

Declerck, J., Subsol G., Thirion, J. P., and Ayache, N. (1995). *Automatic Retrieval of Anatomical Structurers in 3D Medical Images*. INRIA Technical Report **2485**, 153–162.

Drury H. A., van Essen, D. C., Anderson, C. H., Lee, C. W., Coogan, T. A., and Lewis, J. W. (1996). Computerized mapping of the cerebral cortex, a multiresolution flattening method and a surface-based coordinate system. *J. Cog. Neurosci*. **8(1)**, 1–28.

Evans, A. C., Collins, D. L., and Holmes, C. J. (1996). Computational approaches to quantifying human neuroanatomic variability. In *Brain Mapping*, The Methods (Toga, A. W., and Mazziotta, J. C., Eds.). New York Academic Press, New York.

Evans, A. C., Collins, D. L., Neelin, P., MacDonald, D., Kamber, M., Marrett, T. S. (1994). Three-dimensional correlative imaging, applications in human brain mapping. In *Functional Neuroimaging*, Technical Foundations. (Thatcher, R. W., Hallett, M., Zeffiro, T., John, E. R., and Huerta, M., Eds.), Academic Press, Orlando, FL, pp. 145–162.

Evans, A. C., Collins, D. L., and Milner, B. (1992). An MRI-based stereotactic brain atlas from 300 young normal subjects. In *Proceedings of the 22nd Annual Symposium of the Society of Neuroscience* Anaheim, CA, p. 408.

Evans, A. C., Marrett, S., Torrescorzo, J., Ku, S., and Collins, L. (1991). MRI-PET correlation in three dimensions using a volume of interest (VOI). atlas. *J. Cereb. Blood Flow Metab*. **11**, A69–A78.

Fox, P., Perlmutter, J., and Raichle, M. (1985). A stereotactic method of anatomical localization for PET. *J. Comput. Assisted Tomogr*. **9**, 141–153.

Franke, R. (1979). *A Critical Comparison of Some Methods for Interpolation of Scattered Data*. Naval Postgraduate School Technical Report NPS-53–79–003.

Friston, K. J., Ashburner, J., Frith, C. D., Pline, J. B., Heather, J. D., and Frackowiak, R. S. (1995). Spatial registration and normalization of images. *Human Brain Mapping* **2**, 165–189.

Friston, K. J., Frith, C. D., Liddle, P. F, and Frackowiak, R. S. (1991). Plastic transformation of PET images. *J. Comput. Assisted Tomogr* **15(4)**, 634–639.

Gambo-Aldeco, A., and Fellingham L. (1986). Correlation of 3D surfaces from multiple modalities in medical imaging. In *Medical Imaging, Processing, and Display and Picture Archiving and Communication Systems for Medical Applications*. SPIE Medicine XIV/ PACS IV, February, Newport Beach, CA.

Gourdon, A., and Ayache, N. (1994). *Registration of a Curve on a Surface using Differential Properties*. INRIA Internal Report No. **2145**, 187–192.

Greitz, T., Bohm, C., Holte, S., and Eriksson, L. (1991). A Computerized Brain Atlas, Construction, Anatomical Content and Application. *J. Comp. Assisted Tomogr* **15(1)**, 26–38

Gueziec, A., and Ayache, N. (1992). Smoothing and matching of 3D space curves. In *Proceedings of the European Conference on Computer Vision*. [AU21]pp 620–629.

Haar, B. M. *et al*. (1993). Higher order differential structure of images. In *Proceedings of the 13th International Conference on Information Processing in Medical Images* (Barrett, H. H., and Gmitro, A. F., Eds.), 77–93.

Haar, B. M., Florack, L. M. J., Koenderink, J. J., and Viergever, M. A. (1991). Scale-space, its natural operators and differential invariants. In *Proceedings of the 12th International Conference on Information Processing in Medical Images* (Colchester, A. C. F., and Hawkes, D. J., Eds.), **511**, pp. 239–253.

Hardy R. L. (1990). Theory and applications of the multiquadric-biharmonic method, 20 years of discovery 1968–1988. *Computers Math. Appl*. **19**, 163–208.

Hill, D. L. G., Hawkes, D. J., Crossman, J. E., Gleeson, M. J., Cox, T. C. S. *et al*. (1991). Registration of MR and CT images for skull base surgery using point-like anatomical features. *Br. J. Radiol*. **64(767)**, 1030–1035.

Hohne, K. H., Bomans, M., Riemer, M., Schubert, R., Tiede, U., and Lierse, W. (1992). A 3D anatomical atlas based on a volume model. *IEEE Comput. Graphics Appl*. **12**, 72–78.

Joshi, S. C., Miller, M. I., Chiristensen, G. E., Banerjee, A., Coogan, T. A., and Grenander, U. (1995). Hierarchical brain mapping via a generalized dirichlet solution for mapping brain manifolds, vision geometry IV. *Proc. SPIE Conf. Optical Sci. Engin. Instr*. **2573**, 278–289

Kendall, D. G. (1984). Shape-manifolds, Procrustean metrics, and complex projective spaces. *Bull. London Math. Soc*. **16**, 81–121.

Kikinis, R., Shenton, M. E., Iosifescu, D. V., McCarley, R. W., Saivironporn, P., Hokama, H. H., Robatino, A., Metcalf, D., Wible, C. G., Portas, C. M., Donnino, R., and Jolesz, F. (1996). A digital brain atlas for surgical planning. model-driven segmentation, and teaching. *IEEE Trans. Visualization Comp. Graphics*. **2(3)**, 232–241

Kishon, E., Hastie, T., and Wolfson, H. (1991). 3-D curve matching using splines. *J. Robotic Syst*. **6(8)**, 723–743.

Kovacic, S., Gee, J. C., Ching, W. S. L., Reivich, M., and Bajcsy, R. (1989). Three-dimensional Registration of PET and CT images. In *Proc. Ann. Int. Conf. IEEE Eng. Med. Biol. Soc*. Vol 11. IEEE Computer Society Press, Los Alamitos, CA, pp. 548–549.

MacDonald, D., Avis, D., and Evans, A. C. (1993). Automatic parameterization of human cortical surfaces. *Annual Symp. Info. Proc. in Med. Imag. (IPMI)*.

Maguire, G. Q., Noz, M., Rusinek, H., Jaeger, J., Kramer, E. L., Sanger, J. J., and Smith, G. (1991). Graphics applied to medical image registration. *IEEE Comp. Graphics Appl*. **11**, 20–28.

Maguire, G. Q., Noz, M. E., Lee, E. M., and Schimpf, J. H. (1986). Correlation methods for tomographic images using two and three dimensional techniques. In *Information Processing in Medical Imaging* (Bacharach, S. L., Ed.). Martinus Nijhoff, Dordrecht, pp. 266–279.

Maintz, J. B. A., and Viergever, M. A. (1998). *A Survey of Medical Image Registration Medical Image Analysis* **2(1)**, 1–36.

Maurer, C. R., and Fitzpatrick, J. M. (1993). A review of medical image registration. In *Interactive Image-Guided Neurosurgery* (Maciunas, R. J., Ed.). American Association of Neurological Surgeons, Parkridge, IL, pp. 17–44.

Matsui T., and Hirano, A. (1978). *An Atlas of the Human Brain for Computerized Tomography*. Igako-Shoin.

Mazziotta, J. C., Toga, A. W., Evans, A. C., Fox, P., and Lancaster, J. (1995). A probabilistic atlas of the human brain, theory and rationale for its development. *NeuroImage* **2**, 89–101

Meyer, C. R., Leichtman, G. S., Brunberg, J. A., Wahl, R. L., and Quint, L. E. (1995). Simultaneous usage of homologous points, lines and planes for optimal 3-D linear registration of multimodality imaging data. *IEEE Trans. Med. Imaging* **14**, 1–11.

Miller, M. I., Christensen, G. E., Amit, Y., and Grenander, U. (1993). Mathematical textbook of deformable neuroanatomies. *Proc. Nat. Acad. Sci*. **90(24),** 11944–11948.

Nowinski, W. L., Fang, A., Nguyen, B. T., Raphel, J. K., Jagannathan, L., Raghavan, R., Bryan, R. N., and Miller, G. (1997). Multiple brain atlas database and atlas-based neuroimaging system. *J. Image Guided Surgery* **2(1),** 42–66.

Ono M., Kubik S., and Abernathey C. D. (1990). *Atlas of the Cerebral Sulci*. Thieme Medical Publishers, Stuttgart.

Payne, B. A., and Toga, A. W. (1990). Surface mapping brain function on 3D models. *IEEE Comp. Graphics Appl*. **10**, 33–41.

Paxinos, G., and Watson, C. (1986). *The Rat Brain in Stereotaxic Coordinates*. Academic Press, San Diego, CA.

Pelizzari, C., Chen, G., Sperling, D., Weichselbaum, R., and Chen, C. (1989). Accurate three-dimensional registration of CT, PET, and/or MRI images of the brain. *J. Comp. Assisted Tomogr* **13**, 20–26.

Rademacher, J., Caviness, V. S., Steinmetz, H., and Galaburda, A. M. (1993). Topographic variation of the human primary cortices, implications for neuroimaging, brain mapping and neurobiology. *Cerebral Cortex* **3(4)**, 313–329.

Rohlf, F. J., and Slice, D. (1990). Extensions of the Procrustes method for the optimal superposition of landmarks. *Systematic Zool*. **39**, 40–59

Ruprecht, D., and Muller, H. (1995). A framework for scattered data interpolation. In *Visualization in Scientific Computing* (Goebel, M., Muller, H., and Urban, B., Eds.). Springer-Verlag, Vienna.

Sandor, S. R., and Leahy, R. M. (1995). Towards automated labeling of the cerebral cortex using a deformable atlas. In *Info. Proc. in Med. Imag*. [AU30] (Bizais, Y., Barillot, C., and Di Poala, R., Eds.), June. pp. 127–138.

Schaltenbrand, G., and Bailey. P. (1959). *Introduction to Stereotaxis with an Atlas of Human Brain*. Stuttgart, New York.

Schaltenbrand, G., and Wahren, W. (1977). *Atlas for Stereotaxy of the Human Brain*. Georg Thieme Verlag, Stuttgart.

Sokolnikoff, I. S. (1956). *Mathematical Theory of Elasticity*. McGraw-Hill, New York.

Spritzer, V., Ackerman M. J., Scherzinger, A. L., and Whitlock, D. (1996). The visible human male, a technical report. *J. Am. Med. Informatics Assoc*. **3(2)**, 118–130.

Steinmetz, H., Furst, G., and Freund, H. J. (1989). Cerebral cortical localization, application and validation of the proportional grid system in magnetic resonance imaging. *J. Comp. Assisted Tomogr*. **13**, 10–19.

Strother, S. C., Anderson, J. R., Xu, X. L., Liow, J. S., Bonar, D. C., and Rottenberg, D. A. (1994). Quantitative comparisons of image registration techniques based on high-resolution MRI of the brain. *J. Comp. Assisted Tomogr*. **18**, 954–62.

Swanson, L. W. (1992). *Brain Maps*, Structure of the Rat Brain. Elsevier Science, New York.

Szeliski, R., and Lavallee, S. (1994). Matching 3-D anatomical surfaces with non-rigid volumetric deformations. In *Applications of Computer Vision in Medical Image Processing*. Spring Symposium Series, AAAI, Stanford, CA.

Talairach, J., and Szikla, G. (1967). *Atlas d'Anatomie Sterotaxique du Telencephale*, Etudes Anatomo-Radiologiques. Masson & Cie, Paris.

Talairach, J., and Tournoux, P. (1993). *Referentially Oriented Cerebral MRI Anatomy. Atlas of Stereotaxic Anatomical Correlations for Gray and White Matter*. Georg Thieme Verlag, Stuttgart.

Talairach, J., and Tournoux, P. (1988). *Co-Planar Stereotaxic Atlas of the Human Brain*. Georg Thieme Verlag, Stuttgart.

Thompson, P. M., and Toga, A. W. (1996). A surface-based technique for warping three-dimensional images of the brain. *IEEE Trans. Med. Imaging* **15(4)**, 1–16

Thompson, P. M., and Toga, A. W. (1999). Anatomically Driven Strategies for High-Dimensional Brain Image Warping and Pathology Detection. In *Brain Warping* (Toga, A. W., Ed.). Academic Press, New York.

Thurfjell, L., Bohm, C., Greitz, T., and Eriksson, L., (1993). Transformations and slgorithms in a vomputerized brain atlas. *IEEE Trans. Nucl. Sci*. **40(4, pt. 1)**, 1167–91

Tikhonov, A. N., and Arsenin, V. A. (1977). *Solutions of Ill-Posed Problems*. Winston and Sons, Washington, D.C.

Toga, A. W., Santori, E. M., Hazani, R., and Ambach, K. (1995). A 3D digital map of rat brain. *Brain Res. Bull*. **38(1)**, 77–85.

Toga, A. W., and Thompson, P. M. (1999). Multimodal Brain Atlases. In *Advances in Biomedical Image Databases* (Wong, S., Ed.). Kluwer Academic Press, New York.

Vaillant, M., and Davatzikos, C. (1997). Mapping the cerebral sulci, application to morphological analysis of the cortex and to non-rigid registration annual sump. *Info. Proc. Med. Imaging (IPMI)*.

Vaillant, M., and Davatzikos, C. (1996/7), Finding parametric representation of the cortical sulci using an active contour model. *Med. Image Anal*. **1(4)**, 295–315.

van Buren, J., and Maccubbin, D. (1962). An outline atlas of the human basal ganglia with estimation of anatomical variants. *J. Neurosurg.* **19**, 811–839.

van den Elsen, P. A. (1994). Retrospective fusion of CT and MR brain images using mathematical operators. In *Applications of Computer Vision in Medical Image Processing*. Spring Symposium Series, AAAI. Stanford University, Stanford, CA, pp. 30–33.

van den Elsen, P. A. (1992). Multimodality Matching of Brain Images, PhD thesis. Utrecht University, The Netherlands.

van den Elsen, P. A., Pol, E. J. D., and Viergever, M. A. (1993). Medical image matching a review with classification. *IEEE Eng. Med. Biol.* **12**, 26–39.

Vries, J., and McLinden, S. (1988). Computerized three-dimensional stereotactic atlases. In *Modern Stereotactic Neurosurgery*. Little Brown & Company, Boston.

Vvedensky D. D., and Holloway, S. (1992). *Graphics and Animation in Surface Science*. Adam Hilger, UK.

Woods, R. P., Mazziotta, J. C., and Cherry, S. (1993). MRI-PET registration with automated algorithm. *J. Comp. Assisted Tomogr.* **17(4)**, 536–546.

Woods, R. P., Cherry, S. R., and Mazziotta, J. C. (1992). Rapid automated algorithm for aligning and reslicing PET images. *J. Comp. Assisted Tomogr.* **16(4)**, 620–633.

Xu, C., and Prince, J. L. (1997). Gradient vector flow, a new external force for snakes. In *IEEE Proc. CVPR*. Computer Society Press[AU35], Los Alamitos, pp. 66–71.